ELECTROCHEMICAL STUDY ABOUT ZINC ELECTRODEPOSITION ONTO GCE AND HOPG SUBSTRATES

Madai Granados-Neri, Luis Humberto Mendoza Huizar* y Clara Hilda Rios-Reyes
Área Académica de Química, Universidad Autónoma del Estado de Hidalgo, Mineral de la Reforma, CP 42186, Hidalgo, México

We carried out an electrochemical study about zinc electrodeposition onto GCE and HOPG substrates from an electrolytic plating bath containing 0.01M $ZnSO_4$ + 1M $(NH_4)_2SO_4$ at pH 7. Under our experimental conditions the predominant chemical species was the complex $[ZnSO_4(H_2O)_5]$. The chronoamperometric study showed that zinc electrodeposition follows a typical 3D nucleation mechanism in both substrates. The average ΔG calculated for the stable nucleus formation was 6.92×10^{-21} J nuclei^{-1} and 1.35×10^{-20} J nuclei^{-1} for GCE and HOPG, respectively. The scanning electron microscopy (SEM) images showed different nucleation and growth processes on GCE and HOPG substrates at same overpotential.

Keywords: zinc; electrodeposition; carbon.

INTRODUCTION

Zinc electrodeposits are used in many applications to improve the corrosion resistance and several factors influence their electrodeposition. It has been reported that different morphologies and textures of zinc electrodeposits may be obtained by changing electrochemical deposition parameters. These parameters are current density, temperature, pH, substrate surface preparation and bath composition.[1-5] However, despite its great significance to the plating industry, often the nucleation and crystal growth process it is not well understood. Although, the zinc electrodeposition is well recognized, the kinetic parameters related to this are unclear yet. Some reports in the literature propose that the zinc electrodeposition is fast, autocatalytic and controlled by electronic transfer charge[2,6-8] other reports suggest a diffusion control.[9-11] Only few works report the nucleation parameters associated with zinc electrodeposition, especially on carbon substrates.[2,12-14] Probably, the main advantage of use carbon electrodes in the electrodeposition studies, is that it is an inert substrate, and it is possible to study nucleation and growth neglecting the metal-metal interaction.

Trejo *et al*. found that zinc electrodeposition onto glassy carbon electrode (GCE) changes from instantaneous to progressive increasing the zinc ions in the bath while the nucleation rate is controlled by transfer charge.[15] Yu *et al*. reported a zinc instantaneous nucleation from acetate baths on GCE with a deviation to progressive nucleation when the potential applied is increased.[16] Sonneveld *et al*. found an instantaneous nucleation with a hemiespherical 3D growth on GCE from zincate solutions.[14] On the other hand, zinc electrodeposition on high oriented pyrolytic graphite (HOPG) electrodes has been few studied.[17,18] Up to our knowledge, a comparison between the kinetic parameters of zinc electrodeposition from ammoniacal sulfate baths onto GCE and HOPG is missing. Thus, in this paper, a kinetical study of the zinc electrodeposition onto GCE and HOPG electrodes from ammoniacal sulfate baths is examined. Electrochemical techniques such as cyclic voltammetry, chronoamperometry were employed. Scanning electron microscopy was used to analyze the deposits obtained.

EXPERIMENTAL

Zinc electrodeposits onto GCE and HOPG electrodes were carried out from an aqueous solution containing 0.01M $ZnSO_4$ + 1M $(NH_4)_2SO_4$ at pH 7 (natural pH) at 25 °C. All solutions were prepared using analytic grade reagents with ultra pure water (Millipore-Q system) and were deoxygenated by bubbling N_2 for 15 min before each experiment. Once the solution was deoxygenated a nitrogen atmosphere was maintained over the solution. The bubbling was stopped to avoid the presence of additional diffusional variables caused by the nitrogen bubbles on the electrode surface. The working electrodes were a GCE tip provided by BAS™ with 0.071 cm^2 and a freshly cleaved HOPG surfaces. In the case of GCE, the exposed surface was polished to a mirror finish with different grades of alumina down to 0.05 μm and ultrasonically cleaned before experiments. A graphite bar with an exposed area greater than the working electrode was used as counter electrode. A saturated calomel electrode (SCE) was used as reference electrode, with all measured potentials referred to this scale. The electrochemical experiments were carried out in a BAS potentiostat connected to a personal computer running the BAS100 W software to allow the control of experiments and data acquisition. In order to verify the electrochemical behavior of the electrode in the electrodeposition bath, a cyclic voltammetry study was performed in the 0.200 to -1.600 V potential interval at the scan rate range [10-300] mVs^{-1} (Figure 1S, supplementary material). The kinetic mechanism of zinc deposit onto GCE was studied under potentiostatic conditions by the analysis of the experimental current density transients obtained with the potential step technique. The perturbation of the potential electrode always started at 0.200 V. The potential step was imposed at different potentials detailed in this work. Microstructures of electrodeposits were examined by using a scanning electron microscope (SEM; JEOL6300).

RESULTS AND DISCUSSION

Voltammetric study

To establish the chemical species in the deposition bath and the equilibrium potential under our experimental conditions, we perfor-

*e-mail: hhuizar@uaeh.edu.mx

med a thermodynamic study by employing the multicomponent Pourbaix diagrams.[19] The equilibrium constants of the different chemical processes associated to these species were obtained from literature.[20] The speciation of Zn in solution was examined by constructing the distribution–pH diagrams. The results are shown in Figure 1. Note that under our experimental conditions the predominant chemical species is a zinc sulfate complex $[ZnSO_4(H_2O)]_5$. From Pourbaix diagram, the potential of the $[ZnSO_4(H_2O)]_5/Zn$ couple was determined as -1.148 V vs SCE.

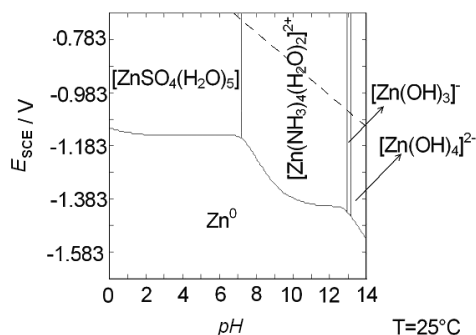**Figure 1.** *Pourbaix-type diagrams of the Zn(II)/Zn(0) systems, pZn(II)''=2.0, pSO4'=0.0 and pNH3'=-0.3*

Figure 2 shows the typical voltammetric responses, at the scan rate of 140 mVs⁻¹, obtained from GCE/10−2M of $ZnSO_4$ + 1 M $(NH_4)_2SO_4$ (system I) and HOPG/10^{-2} M of $ZnSO_4$ + 1 M $(NH_4)_2SO_4$ (system II) systems. For both systems, it was recorded at direct scan, the formation of peaks a and a′ at −1.355 and -1.405 V, respectively. During the inverse of the potential scan, it is possible to observe the crossovers, E_{C1}, E_{C2} which are typical of the formation of a new phase involving a nucleation process.[21] Others crossoverpotentials were detected at -1.161 and -1.143 V for system I and II respectively. Note that these potentials were recorded at a null current value, in where the equilibrium given by Equation 1 is expected.
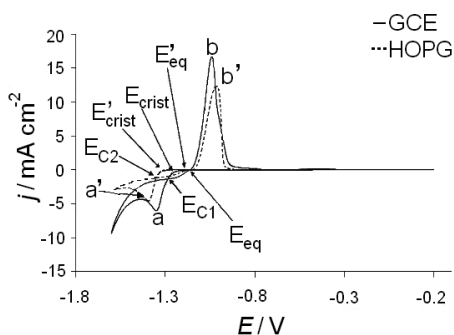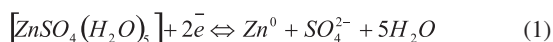
$$\left[ZnSO_4\left(H_2O\right)_5\right] + 2\bar{e} \Leftrightarrow Zn^0 + SO_4^{2-} + 5H_2O \qquad (1)$$

Figure 2. *A comparison of two cyclic voltammetric curves obtained in the GCE (solid line) and HOPG (broken line) from an aqueous solution 10^{-2} M of $ZnSO_4$ and 1 M $(NH_4)_2SO_4$ (pH 7.0). The potential scan rate was started at 0.600 V toward the negative direction with a potential scan rate of 140 mV s⁻¹*

Note that these values of E_{eq} and E'_{eq} compare favorably with the equilibrium potential calculated from Pourbaix's diagrams. Also, it is shown the zinc electrodeposition process starts at −1.240 V (E_{crist}) and −1.316 V (E_{crist}) for systems I and II, respectively. Last results suggest that, the energetic cost to perform the zinc electrodeposition is favored onto GCE in comparison with the HOPG substrate. In the anodic zone, it was possible to observe two principal peaks b and

b′ at −1.031 and -1.052 V, respectively. To determine the control limiting of the zinc electrodeposition process, the current density (j_p) value associated with both peaks a and a′ was plotted as a function of $v^{1/2}$ (Figure 1S, supplementary material). A linear relationship was found for both cases, according to the Berzins-Delahay equation,[22, 23] suggesting a diffusional control of the zinc electrodeposition process.

Choronoamperometric study

Formation of new phases occurs through nucleation and growth mechanisms in where information about the electrocrystallization process can be obtained from potentiostatic studies. Figure 3a-b shows a set of density current transients recorded at different potentials by potential step technique from systems I and II.
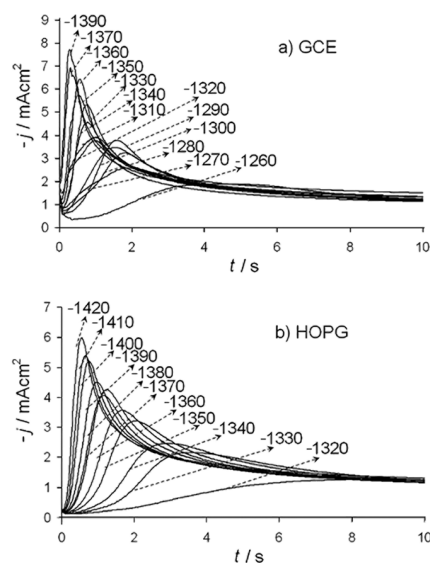

Figure 3. *A set of current transients obtained from aqueous solution 10^{-2} M of $ZnSO_4$ and 1 M $(NH_4)_2SO_4$ (pH 7.0) on a) GCE and b) HOPG electrodes by means of the potential step technique for different potential step values (mV) indicated in the figure. In all the cases, the initial potential was 0.600 V*

These transients were obtained by applying an initial potential of 0.200 V on the surface of the carbon electrode. At this potential value, the zinc deposition had not still begun (Figures 1 and 2). After the application of this initial potential, a step of negative potential (E_c) was varied on the surface of the electrode for 32 s. All transients showed a typical current maximum (j_m) which is characteristic of a three-dimensional nucleation process with hemispherical diffusion control (3D-dc).[10,11] A classification of the nucleation as instantaneous or progressive from transients it is possible by following the criteria established by Sharifker *et al.*[10] in where the experimental transients in a nondimensional form by plotting j^2/j_m^2 vs t/t_m are compared to those theoretically generated from Equations 2 and 3 for instantaneous and progressive nucleation, respectively.

$$\frac{j^2}{j_m^2} = 1.9254\left(\frac{t}{t_m}\right)^{-1}\left\{1 - \exp\left[-1.2564\left(\frac{t}{t_m}\right)\right]\right\}^2 \qquad (2)$$

$$\frac{j^2}{j_m^2} = 1.2254\left(\frac{t}{t_m}\right)^{-1}\left\{1 - \exp\left[-2.3367\left(\frac{t}{t_m}\right)^2\right]\right\}^2 \qquad (3)$$

The comparison of the theoretical dimensionless transients, generated by Equations 2 and 3 with the experimental dimensionless current transients (Figure 2S, supplementary material), suggested that

the experimental curves closely follows the response predicted for a 3D progressive nucleation. This behavior may be expected because our system contains ammonium and sulfate ions. Thus, it has been reported that sulfate anion induces a competitive adsorption effect on the substrate complicating the electrodeposition process,[24,25] which can induce a progressive nucleation mechanism. Moreover, NH_4^+ ions may preferentially adsorb on certain orientations too, delaying the nucleation rate.[26]

It has been proposed that the diffusion-limited 3D growth of metallic centers can be predicted by:[27]

$$j_{3D} = \frac{zFDc_0}{(\pi Dt)^{1/2}} \frac{\Phi}{\Theta} \left\{1 - \exp\left[-bt\Theta\right]\right\} \tag{4}$$

where:

$$b = (2\pi)^{3/2} D (Mc_0/\rho)^{1/2} N_0 \tag{5}$$

$$\Theta = 1 - \left(1 - e^{-At}\right)/At \tag{6}$$

$$\Phi = 1 - \frac{e^{-At}}{(At)^{1/2}} \int_0^{(At)^{1/2}} e^{\lambda^2} d\lambda = 1 - \frac{1}{(At)^{1/2}} \left(\frac{0.051314213 + 0.47910725(At)^{1/2}}{1 - 1.2068142(At)^{1/2} + 1.185724(At)} \right) \tag{7}$$

where N_0 is the number of active nucleation sites, A is the nucleation rate. Here, it must be mentioned that N_0 and A are potential dependent and an increasing of these quantities is expected with the decrease of the potential applied. D is the diffusion coefficient, F is the Faraday's constant and all others parameters have their conventional meanings.

Figure 4 shows a typical comparison of the reduction experimental current transients, with the theoretically generated by nonlinear fitting of experimental data to Equation 4. It can be observed that the model expressed by this equation adequately accounted for the behavior of experimental transient.
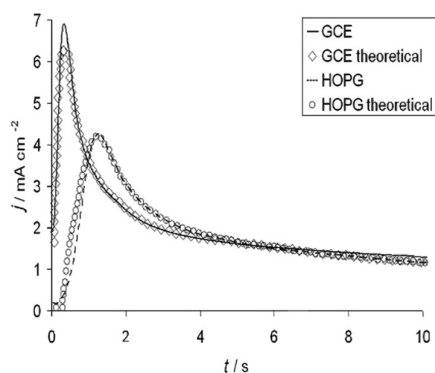

Figure 4. Comparison between an experimental current density transients (—) recorded during the zinc electrodeposition onto GCE (a) and HOPG (b) electrodes when a potential value of −1.320 V was applied with a theoretical transient (◊, GCE) and (O,HOPG) generated by non-linear fitting of Equation 4

The physical parameters obtained from the adjustments of Equation 4 are reported in present work (Table 1). It can be seen that an increment of A and N_0 is obtained when the overpotential applied is increased. Also, observe that the nucleation rate is bigger on GCE than on HOPG, the same behavior can be observed in the number of active nucleation sites. This situation can be explained due to the presence of more structural defects on GCE surface than the obtained on HOPG electrode.

Table 1. Potential dependence for the nucleation parameters during Zn electrodeposition onto GCE and HOPG electrodes from aqueous solution containing 10^{-2} M of $ZnSO_4 + 1M$ $(NH_4)_2SO_4$. The values were obtained from best-fit parameters found through the fitting process of the experimental j-t plots using Equation 4

-E (V)	GCE			HOPG		
	A / s^{-1}cm^2	$DX10^5$ / cm^2 s^{-1}	N_0X10^{-6} / cm^2	A / cm^2 s^{-1}	$DX10^5$ / cm^2 s^{-1}	N_0X10^{-6} / cm^2
1.26	0.568	1.112	0.489	0.019	0.769	0.030
1.27	0.681	1.094	0.905	0.022	0.919	0.039
1.28	0.785	1.140	1.066	0.028	0.919	0.056
1.29	0.795	1.108	1.508	0.031	0.919	0.115
1.30	1.085	1.125	1.545	0.035	0.916	0.267
1.31	1.303	1.036	4.621	0.046	0.987	0.421
1.32	1.237	1.076	3.790	0.241	1.290	0.151
1.33	1.709	0.919	11.013	0.647	1.082	0.612
1.34	1.894	1.019	2.624	0.754	1.061	0.838
1.35	3.506	1.365	2.264	1.179	1.073	1.333
1.36	3.050	1.413	2.426	1.249	1.099	1.488
1.37	4.128	0.992	21.966	0.141	0.793	11.595
1.39	4.853	1.230	18.285	0.207	0.843	10.765

Table 2. Potential dependence of the N_s from aqueous solution containing 10^{-2} M of $ZnSO_4 + 1$ M $(NH_4)_2SO_4$ calculated from physical constants reported in Table 1 and Equation 8

-E / V	GCE N_sX10^{-6} (cm^2)	HOPG N_sX10^{-6} (cm^2)
1.260	0.414	0.028
1.270	0.928	0.031
1.280	0.987	0.042
1.290	1.133	0.062
1.300	1.197	0.103
1.310	2.156	0.143
1.320	1.916	0.171
1.330	1.455	0.617
1.340	2.611	0.788
1.350	2.863	1.235
1.360	2.465	1.328
1.370	3.254	1.467
1.390	2.796	2.475

Through the physical constants reported, it was also possible to calculate the saturation number of nuclei (Ns) (Table 2). This estimation was made by using Equation 8:[10]

$$N_S = \left(\frac{AN_0}{2k'D}\right)^{1/2} \tag{8}$$

where

$$k' = \frac{4}{3} \left(\frac{8\pi C_o M}{\rho}\right)^{1/2} \tag{9}$$

Observe the N_s values increased with the applied potential. It is important to mention that, due to the exclusion zones of the deposit, caused by the hemispherical diffusional gradients of 3D nucleus, the N_s will be always lower than the N_0 values at the same applied potential, and both grow in accordance with a more negative potential. Also, from the nucleation rate values reported (Table 1), it is possible to calculate the Gibbs free energy of nucleation employing the next equation:[28]

$$\Delta G = -\frac{k_B T}{\eta^2} \frac{d \ln\left(M_{3d}^{da}\right)}{d\eta^{-2}} = -\frac{k_B T}{\eta^2} \frac{d\left(\ln\left[A \exp\left(\frac{\alpha z e \eta}{k_B T}\right)\right]\right)}{d\eta^{-2}} \quad (10)$$

with

$$M_{3d}^{da} = A \exp\left(\frac{\alpha z e \eta}{k_B T}\right) \quad (11)$$

where ΔG is the Gibbs free energy of nucleation, J/nuclei; k_B is the Boltzmann constant (1.38066×10^{-23} J mol^{-1}), T is the absolute temperature, K, η is the overpotential, z is the charge transferred during the zinc reduction process and e is the elementary charge of the electron. On the other hand, the critical nuclei can be calculated employing:[28]

$$n_c = -\frac{2k_B T}{z e \eta^3} \frac{d\left(\ln\left[A_3' \exp\left(\frac{\alpha z e \eta}{k_B T}\right)\right]\right)}{d\eta^{-2}} = \frac{2\Delta G}{z e \eta} \quad (12)$$

It is important to mention that Equations 10 and 12 are valid in the case of a direct attachment mechanism. The plot $\ln (M_{3d}^d)$ vs η^{-2} showed a linear tendency with a $d(\ln (M_{3d}^d))/d\eta = 3.56 \times 10^{-2}$ and $d(\ln(M_{3d}^d))/d\eta = 6.92 \times 10^{-2}$ for GCE and HOPG respectively. Thus, the ΔG calculated for these systems was 6.92×10^{-21} J/nuclei for GCE substrate while the value calculated for HOPG was 1.35×10^{-20} J/nuclei. These energies correspond to the ΔG value requirements for forming a stable nucleus, the average critical cluster´s size (n_c) calculated employing Equation 10 was n_c=0.326 and n_c=0.634 which cannot be possible because a critical cluster´s size with a fractional number implies the atoms that build the critical nuclei may be divided in fractions. Thus, for example, a n_c= 0.326 indicates that only 0.326 atoms are forming the critical nuclei. Thus, from a physical point of view it is not possible to separate an atom in fractions. This result is because of that in the classical nucleation theory are considered macroscopic parameters which are not adequate to determine atomic quantities without error.[28] Thus, it is better to estimate the critical size of the zinc nucleus in the framework of the atomistic theory of electrolytic nucleation through the following equation:[29]

$$n_c = \left(\frac{k_B T}{z e_0}\right) \frac{d\left(\ln\left[A \exp\left(\frac{\alpha z e \eta}{k_B T}\right)\right]\right)}{d\eta} \quad (13)$$

where α is the transfer coefficient for zinc reduction. The plots $\ln A$ vs. η showed a linear tendency (Figure 3S, supplementary material). The values of $d(\ln A)/dE$ were 24.01 and 50.36 for systems I and II, respectively. Thus, in both substrates, the critical cluster's size calculated was n_c=0. This value means that each active site is a critical nucleus.

Morphological analysis

The morphology of the electrodeposits was studied by SEM. SEM micrographs of an electrodeposit formed potentiostatically at -1.3 V

is shown in Figure 5. Observe that the microstructure and surface morphology of the electrodeposits on GCE were more compact with a finer grain size (200 nm) than the obtained on HOPG; in where the deposits consisted of bigger dispersed particles (400 nm). In both cases, zinc clusters had a spherical microstructure.
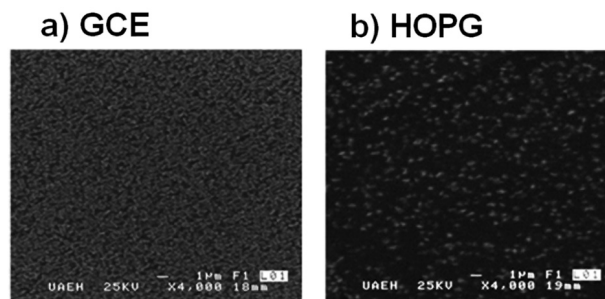

Figure 5. SEM images of the deposits obtained at −1.300 V on a) GCE and b) HOPG, from an aqueous solution 10^{-2} M of $ZnSO_4$ and 1 M $(NH_4)_2SO_4$ (pH 7.0) 4,000× magnification was used

Also, it is possible to observe that on GCE, Figure 5a, a major amount of nuclei was obtained with respect to HOPG substrate. The increase in the nuclei number on GCE probably is because of an increment of the active nucleation sites compared to those obtained on HOPG. These facts suggest that, at same overpotential, the zinc cluster and their number depend on the carbon substrate and the energetic conditions. Thus, the zinc cluster formation is more favorable on GCE than HOPG probably due to the presence of structural defects.

CONCLUSIONS

We carried out an electrochemical study about zinc electrodeposition onto GCE and HOPG substrates from an electrolytic plating bath containing 0.01M $ZnSO_4$ + 1M $(NH_4)_2SO_4$ at pH 7. The analysis of the density current transients showed that the zinc electrodeposition is a diffusion-controlled process with a typical 3D nucleation mechanism in GCE and HOPG. The average ΔG calculated for the stable nucleus formation was 6.92×10^{-21} J nuclei^{-1} and 1.35×10^{-20} J nuclei^{-1} for GCE and HOPG, respectively. The SEM images showed the formation of bigger nuclei onto HOPG (400 nm) in comparison with those obtained onto GCE (200nm).

SUPPLEMENTARY MATERIAL

Available on http://quimicanova.sbq.org.br, in pdf file, with free access.

REFERENCES

1. Raeissi, K.; Saatchi, A.; Golozar, M. A.; Szpunar, J. A.; *J. Appl. Electrochem.* **2004**, *34*, 1249.
2. Mendoza-Huizar, L. H.; Rios-Reyes, C. H.; Gómez-Villegas, M. G.; *J. Mex. Chem. Soc.* **2009**, *53*, 243.

3. Younan, N. M.; *J. Appl. Electrochem.* **2000**, *30*, 55.

4. Millet, J. P.; Gravria, M.; Mazille, H.; Marchandise, D.; Cuntz, J. M.; *Surf. Coat. Technol*. **2000**, *123*, 164.

5. Lin, C. S.; Lee, H. B.; Hsieh, S. H.; *Metall. Trans. A* **2000**, *31A*, 475.

6. Vasilakopoulos, D. ; Bouroushian, M. ; Spyrellis, N. ; *Electrochim. Acta* **2009**, *54*, 2509.

7. Elpelboin, I.; Ksouri, M.; Wiart, R.; *Faraday Disc. Chem Soc.* **1978**, *12*, 115.

8. Weil, R.; *Annu. Rev. Mater. Sci*. **1989**, *19*, 165.

9. Sonneveld, P. J.; Visscher, W.; Barendrecht, E.; *Electrochim Acta* **1992**, *37*, 1199.

10. Scharifker, B. R.; Hills, G.; *Electrochim. Acta* **1983**, *28*, 879.

11. Scharifker, B. R.; Mostany, J.; *J. Electroanal. Chem.* **1984**, *177*, 13.

12. Raeissi, K.; Saatchi, A.; Golozar, M. A.; *J. Appl. Electrochem.* **2003**, *33*, 635.

13. Yu, J.; Yang, H.; Ai, X.; Chen, Y.; *Russ. J. Electrochem.* **2002**, *38*, 321.

14. Torrent-Burgue, J.; Guaus, E.; *J. Appl. Electrochem.* **2007**, *37*, 643.

15. Trejo, G.; Ortega, R.; Meas, Y.; Ozil, P.; Chainet, E.; Nguyen, B.; *J. Electrochem. Soc.* **1998**, *145*, 4090.

16. Yu, J.; Cao, H.; Chen, Y.; Kang, L.; Yang, H.; *J. Electroanal. Chem.* **1999**, *474*, 69.

17. Kryshtop, I.; Yurchenko, N.; Trofimenko, V.; *ECS Transactions* **2008**, *13*, 65.

18. Alvarez, A. E.; Salinas, D. R.; *J. Electroanal. Chem.* **2004**, *566*, 393.

19. Rojas-Hernández, A.; Ramírez, T. M.; Ibáñez, J. G.; González I.; *J. Electrochem. Soc.* **1991**, *138*, 365.

20. Puigdomenech, I.; *Hydra/Medusa Chemical Equilibrium Database and Plotting Software* 2004, KTH Royal Institute of Technology, freely downloadable software at http://www.kemi.kth.se/medusa. accessed in March 2010.

21. Greef, R.; Peat, R.; Peter, L. M.; Pletcher, D.; Robinson, J.; *Instrumental Methods in Electrochemistry*, Ellis Horwood: Chichester, 1985, ch. 9.

22. Berzins, T.; Delahay, P.; *J. Am. Chem. Soc.* **1953**, *75*, 555.

23. Delahay, P.; *New Instrumental Methods in Electrochemistry*, Interscience: New York, 1954, p. 122.

24. Wheeler, D. R.; Wang, J. X.; Adzic, R. R.; *J. Electroanal. Chem.* **1995**, *387*, 115.

25. Jia-Wei, Y.; Jian-Ming, W.; Wu, Q.; Zhao-Xiong, X.; Bing-Wei, M.; *Langmuir* **2003**, *19*, 7948.

26. Bertazzoli, R.; Sousa, A. D. F. B.; *J. Braz. Chem. Soc.* **1997**, *8*, 357.

27. Heerman, L.; Tarallo, A.; *Electrochem. Commun*. **2000**, *2*, 85.

28. Milchev, A.; *Electrocrystallization: Fundamentals of nucleation and growth*, Kluwer Academic Publishers: Massachusetts, 2002, ch. 2.2.3.

29. Milchev, A.; *Contemp. Phys.* **1991**, *32*, 321.